Plant Physiol. (1981) 67, 570–579
0032-0889/81/67/0570/10/$00.50/0

Photosystem II Photosynthetic Unit Sizes from Fluorescence Induction in Leaves[1]

CORRELATION TO PHOTOSYNTHETIC CAPACITY

Received for publication February 26, 1980 and in revised form September 18, 1980

SHMUEL MALKIN[2], PAUL A. ARMOND[3], HAROLD A MOONEY, AND DAVID C. FORK
Department of Plant Biology, Carnegie Institution of Washington, and Department of Biology, Stanford University, Stanford, California 94305

ABSTRACT

The use of fluorescence induction measurements in leaves infiltrated with 3-(3,4-dichlorophenyl)-1,1-dimethylurea has been evaluated as a routine method for estimation of the concentration of the reaction centers of photosystem II relative to total chlorophyll in a wide variety of plant species. The procedure is based on a simple theory that takes into account the attenuation of light in passing through the leaf and the linear dependence of the fluorescence induction time from different parts of the leaf on the inverse of the local light intensity. A formula to calculate the reaction center concentration of photosystem II was obtained. The effect of the light attenuation is accounted for by a correction factor which could become practically insignificant by an optimal choice of the excitation and emission wavelengths and the geometry of the photodetector with respect to the sample. Estimation of quantum yields for primary photochemistry and influence of light scattering were considered. The results demonstrate the effect of the above factors under various circumstances and are in agreement, to a first approximation, with the theory.

The utility of the method is demonstrated by a detailed study of four desert plant species: estimation of reaction center concentrations of both photosystem I (by estimation of P700) and photosystem II (by the fluorescence induction method) were made and were compared to the rates of CO_2 fixation. There was a good quantitative correlation between the photosynthetic rates and the concentration of photosystem II reaction centers (expressed as per chlorophyll or per unit area of the leaf), but no such correlation was found with photosystem I reaction centers.

The ratio of total chlorophyll per reaction centers II varied in the range of about 200 to 800 in different species, but there was no variation of this parameter in any single species.

It is well established that the primary charge transfer processes of photosynthesis take place at reaction centers served by a large number of light-collecting antennae pigments (13, 15, 17, 32, 33, 40) which, in higher plants, consist mainly of Chl *a* and *b*. Knowledge of the number of Chl molecules associated with each reaction center is of considerable importance for understanding the organization and functioning of the antennae pigment complexes serving both PSII and PSI (1, 2, 26, 27, 38). These numbers are probably quite variable in different species of the plant kingdom and in different environments. Since the over-all rate of photosynthesis on a Chl basis may be related to these numbers (39), it follows that they are important in dealing with questions such as the efficiency of photosynthesis (24, 28, 30), including adaptation to the environment [*e.g.* ambient light intensity level (5, 6, 31) or other conditions (3, 7, 23, 37)].

Fluorescence induction in chloroplasts was previously used to obtain the concentration of the PSII electron-acceptor pool (19, 40), as well as the concentration of the reaction centers (10, 11, 40). The principle of the method lies in the equivalence between the number of quanta, which bring about the fluorescence change, and the magnitude of the electron acceptor pool. In the case where DCMU was added, the electron-acceptor pool is limited to the primary acceptor of the reaction center (40), which is therefore computed directly from the fluorescence induction time and the absorbed-light intensity.

It was our aim to develop a method, based on the above principle, which would be applicable, not only to chloroplasts suspensions, but also to leaves. As a technique, clearly this has great advantages, such as rapidity and ease of measurement, coupled with the possibility to scan many plants in a short time. Work with leaves is required for species in which the activity of isolated chloroplasts might be severely impaired during isolation or storage. The greatest difficulty in applying fluorescence induction measurements to leaves is the fact that the light is severely attenuated in passing through the leaf, and the use of a well-defined light intensity, as for the case of dilute chloroplasts suspension is not applicable.

The main purpose here is 2-fold.

First, a modified formula for the fluorescence induction is developed which takes into account the light attenuation by integrating the contributions to the fluorescence from various depths of the leaf. We show how ratios of reaction centers of PSII to the total Chl can be obtained in general.

Second, we applied this formula to analyze fluorescense induction curves of four desert plant species which exhibit distinctly different photosynthetic capacities. A quantitative correlation of photosynthetic rates with the concentration of RC_{II}[4] will be demonstrated.

The implication of our analysis is that either RC_{II} themselves are limiting in the over-all photosynthetic process or, alternatively, a constant stoichiometry exists between RC_{II} and the rate-limiting enzyme(s). Numbers for the ratio of RC_{II} to Chl have been obtained for many plant species to demonstrate the variability of this parameter. Within a single species at specified conditions, the

[1] Carnegie Institution, Department of Plant Biology Publication 669.

[2] On leave from the Biochemistry Department, The Weizmann Institute of Science, Rehovot, Israel.

[3] Supported by a Carnegie Institution of Washington postdoctoral fellowship. Present address: Pfizer Central Research, Eastern Point Road, Groton, CT 06340

[4] Abbreviations: RC_{II}; PSII reaction center(s); PSU, photosynthetic unit.

variability is rather small.

Toward the end of the report given here, there is a somewhat deeper examination of several factors on which the method depends. To test the basic equation based on the light attenuation in the leaf, measurements were made at several wavelengths. We show that the observed fluorescence kinetics are indeed modified significantly by the light attenuation effect and are different at different wavelengths of emission and excitation in agreement with the theory. The effect of light scattering is also examined with the conclusion that in infiltrated leaves it is usually of no crucial importance.

This work is an extension of a previous report (21).

THEORETICAL CONSIDERATIONS

The light-induced rise of Chl-*a* fluorescence from a dark-adapted initial value (F_0) to a maximum value (F_{max}) (fluorescence induction) is believed to reflect the conversion of the primary acceptor (Q) of PSII from an oxidized to a reduced form by the light-induced primary charge separation reaction (19):

$$Q \text{ (low fluorescence } F_0) \xrightarrow{h\nu} Q^- \text{ (high fluorescence } F_{max}) \quad (1)$$

In presence of DCMU, no further electron transport from Q^- is possible, and reaction 1 is limited to the conversion of Q to Q^- alone. To quantitate the fluorescence rise phenomenon, one introduces a quantity $\bar{t}$, defined as the average time of the fluorescence rise, or induction time; it is equal to the time needed for completion of reaction 1 if proceeding with a constant rate equal to its initial rate. The induction time is equal to the area enclosed between the fluorescence curve [$F = F(t)$], the (vertical) axis ($t = 0$), and the maximal fluorescence horizontal line ($F = F_{max}$) when the value $F_{max} - F_0$ is normalized to unity (19).

The total number of photons required to accomplish reaction 1 is estimated by multiplying the rate of photon absorption with the fluorescence induction time ($\bar{t}$). This number, multiplied by the efficiency of the photons, must be stoichiometric with the number of electron transfers which, in the presence of DCMU, is also equal to the number of reaction centers Q. From these considerations, it follows that for a sample unit area incident to a parallel beam of exciting light, the quantity of RC_{II} (in mol) is given by the formula (19):

$$RC_{II} = \alpha_2 \phi_2 I_{abs} \bar{t} \quad (2)$$

where α_2 is the fraction of absorbed light which is absorbed directly by PSII, ϕ_2 is the maximal efficiency of photochemistry in PSII (*i.e.* for open reaction centers), and I_{abs} is the rate of light absorption (expressed in Einsteins per unit area and unit time) by the sample. We shall first apply equation 2 for the idealized case of a very thin sample [of vanishingly small optical path (Δl)] in which the light flux (I) can be considered homogeneous. One can approximately write (Beer-Lambert Law):

$$I_{abs} = (1 - 10^{-\epsilon_i c \Delta l}) I \simeq 2.3 \epsilon_i c I \Delta l \quad (3)$$

where ϵ_i is the molar extinction coefficient for the incident exciting light (averaged for the mixed Chl *a* and *b* population) and c is the total molar concentration of Chl. From equations 2 and 3, one obtains:

$$RC_{II} = 2.3 \alpha_2 \phi_2 \epsilon_i c I \bar{t} \Delta l \quad (4)$$

where $c\Delta l$ is proportional to the total amount of Chl per unit area (If the optical path is expressed in cm, $c\Delta l/1{,}000$ equals the quantity of Chl in mol/cm^2.) Writing (Chl) for the number of mol total Chl in the given sample, one obtains:

$$\frac{RC_{II}}{(Chl)} = 2300 \alpha_2 \phi_2 \epsilon_i I \bar{t} \quad (5)$$

As $RC_{II}/(Chl)$ is a constant property of any given sample from the same source, it can be seen that the induction time ($\bar{t}$), at a given intensity (I), does not depend on the Chl concentration of the sample nor the optical path, as long as the exciting light flux intensity remains uniform.

Consider now that the light intensity is attenuated in passing through a leaf. Each element of different depth will give a different contribution to $\bar{t}$ and to the total fluorescence. The observed induction time is an average of contributions from different depths of the leaf and would be longer than that expected from equation 5 on the basis of the known incident light flux hitting the top layer.

The dependence of $\bar{t}$ on the light flux can be written by the $I \cdot t$ law (19) (also derivable from equation 5)

$$\bar{t} = \frac{I_0 \cdot \bar{t}_0}{I} \quad (6)$$

where I_0 and $\bar{t}_0$ are values for the light intensity and induction time for a specified reference set of conditions (in our case, the top leaf layer) and $\bar{t}$ is the induction time for any other intensity (I).

The observed experimental induction time ($\bar{\tau}$) will be related to $\bar{t}_0$ by taking into account both the attenuation of the incident light (extinction coefficient, ϵ_i), and the fluorescence light (extinction coefficient, ϵ_f) in passing from the place where it is emitted to the photodetector. The calculation is made for the experimental arrangement as shown in Figure 1, where all the parameters are explained. The observed induction time is given by:

$$\bar{\tau} = \bar{t}_0 \left(1 + \frac{\epsilon_i}{\epsilon_f} \cos\theta\right) \quad (7)$$

where θ is the angle that the fluorescence makes with the vertical line (calculated from the photodetector angle and Snell's law) (The calculations are detailed in Appendix I.) The difference between $\bar{\tau}$ and $\bar{t}_0$ is minimal when $(\epsilon_i/\epsilon_f)\cos\theta$ is small compared to 1. This is obtained using wavelength of small ϵ_i (*i.e.* incident light penetrating as much as possible), large ϵ_f (*i.e.* fluorescent light reabsorbed as much as possible), and small $\cos\theta$ (*i.e.* photodetector aligned at a shallow angle to the horizontal). Then $\bar{\tau} \simeq \bar{t}_0$. This approximation is explained qualitatively as follows: inasmuch as fluorescence is considerably reabsorbed, only the contribution

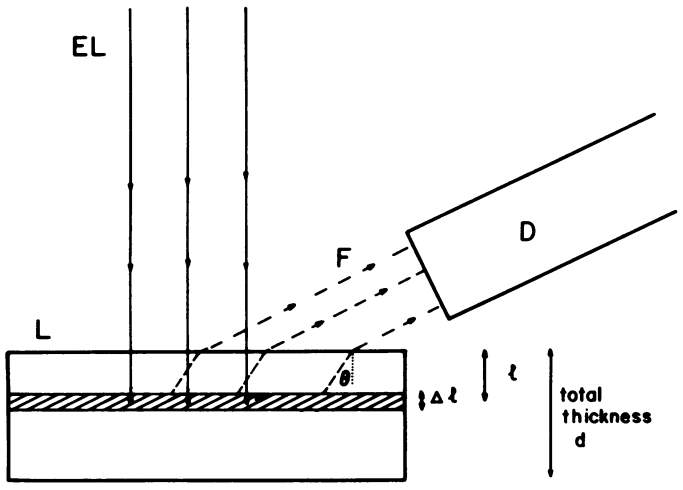

FIG. 1. Experimental arrangement for measuring fluorescence induction of leaves and definition of terms: EL, exciting light; L, leaf; l, variable depth of light penetration through the leaf; d, total thickness of the leaf; D, detector (including filters); F, fluorescence light; θ, angle traversed by the fluorescence in the leaf so that after refraction in the air will reach the detector.

from the uppermost layers is detected, where the exciting light can be regarded as uniform (because it is not yet attenuated to any great extent). Rewriting equation 5 by using the incident flux (I_0) and the induction time ($\bar{t}_0$) appropriate for the top of the leaf and by substituting $\bar{t}_0$ from equation 7, the final result is:

$$\left(\frac{RC_{II}}{Chl}\right) = 2300\ \alpha_2\phi_2\epsilon_i I_0 \frac{\bar{\tau}}{1 + \frac{\epsilon_i}{\epsilon_f}\cos\theta} \quad (8)$$

The reciprocal of RC_{II}/Chl will be referred here as the PSU size of PSII.

In applying equation 8, there is an uncertainty for the numbers that should be adopted for the product $\alpha_2\phi_2$. In isolated chloroplasts, there is an independent method to find the product $\alpha_2\phi_2$ (19) which, for active chloroplasts, yielded a value close to 0.5. However, it is impossible at this stage to estimate $\alpha_2\phi_2$ in leaves by such a method.

A possible approach to estimate ϕ_2 is to assume that it is equal to the excitation trapping efficiency in PSII (20):

$$\phi_2 = 1 - \frac{F_0}{F_{max}} \quad (9)$$

As for α_2, there is no choice at present but to assume a value which will tentatively be considered constant for the higher plant species studied here. This is probably close to the truth as long as the Chl *b*/Chl *a* ratio remains approximately constant. In the absence of any hard data at present, we shall put $\alpha_2 = 0.5$ (even distribution of light in the two photosystems) and correct our numbers in the future if a better evaluation of α_2 is made.[5]

MATERIALS AND METHODS

Leaves from plants grown in garden or greenhouse were vacuum-infiltrated with an aqueous DCMU solution (20 μM). Infiltration is usually successful, if done within 15 s of harvesting, to ensure that the stomata are still opened during infiltration. The concentration of DCMU used was optimal in leaves (in chloroplasts, the required concentration is much less) to inhibit the slow fluorescence, to maintain only fast transients, and to inhibit photosynthesis.

DCMU-infiltrated leaves, water-infiltrated leaves, or untreated leaves (the latter two used as controls) were placed on a flat surface and covered with a flat black cover with a circular opening allowing irradiation of limited exposed area (~1 cm^2). Light from a 500-w quartz iodine lamp was routinely isolated by filters (Corning 4-96, 3-68, 1-60) passing a band around 550 nm (half-band, around 20 nm). A photomultiplier was placed at an angle of approximately 30° to the horizontal. A narrow-band, 685-nm interference filter (5-nm half-band) was used to isolate the fluorescence. The exciting light intensity was routinely determined by a silicon photovoltaic cell, calibrated with a commercial quantum light meter (Li-Cor Incorp., Lincoln, NE; model 185), and also checked with a calibrated thermopile. The use of the above actinic and fluorescence wavelengths and the photomultiplier angle made the correction term $(\epsilon_i/\epsilon_f)\cos\theta$ for the light attenuation effect in the leaf quite small (about 7%).

The opening of a shutter introduced the actinic light onto the surface of the leaf and excited the fluorescence transients. At the same time, it also activated a transient recorder system which stored the fluorescence transient in a digital form. This information was usually recorded in analog form on a X-Y recorder. The induction time was determined by cutting the recorded induction curve and estimating its area by weighing (in comparison to the weight of a standard area). This estimation is accurate to about 10%. In later stages of the work reported here, a computer analysis was introduced giving directly and more precisely computed value for $\bar{t}$ and other parameters as well (14).

Absorbance parameters of leaves and chloroplasts were determined by measurements using an integrating sphere. The *A* data obtained from chloroplasts were used to determine extinction coefficients for Chl *in vivo* (ϵ_i) used in the analysis of fluorescence induction from leaves. To correct for the fact that the integrating sphere is not ideal (apparent), *A* readings were taken at a wavelength which is not absorbed by the chloroplasts (*i.e.* 760 nm). These values were applied for correction of the values obtained at the wavelength of interest, by calculating optical densities and taking the difference. An example of results of such *A* measurements is found in Figure 2. The readings in the integrating sphere showed linearity in the observed optical density and total Chl concentration (Fig. 2) in the convenient range of *A* (about 0.1–0.7). The range of ϵ values at 550 nm was between 8,000 to 11,000. The Chl concentration was determined according to the procedure of Arnon (4).

The four desert plants selected for a special study were *Camissonia brevipes* (Onagraceae), *Lupinus sparsiflorus* (Fabaceae), *Datura meteloides* (Solanaceae) and *Pertityle emoryi* (Asteraceae), all C_3 species. Collected seeds were germinated and grown side by side under a 20 C/15 C day/night temperature regime and a 16-h photoperiod. The response of CO_2 uptake to quantum flux density and CO_2 concentration were determined as previously described (12). P700 concentration was estimated by the method of Shiozawa *et al.* (36) and nitrogen content of the leaf tissue was measured by the Kjeldahl method. All measurements were performed on the plants prior to anthesis.

RESULTS AND DISCUSSION

GENERAL DESCRIPTION OF FLUORESCENCE INDUCTION CHARACTERISTICS

Fluorescence transients from leaves are obtained following an exposure to constant actinic light after a period of dark adaptation. Figure 3 shows examples of such fluorescence transients from control (A), water-infiltrated (B), and DCMU-infiltrated (C) spinach (*Spinacia oleracea*) leaves. In all these transients, there is an artifactual fast rise to an initial level (F_0) limited by the shutter opening time (~3 ms). From F_0, there is a slower (real) rise to a higher fluorescence level. With DCMU, this rise takes much less

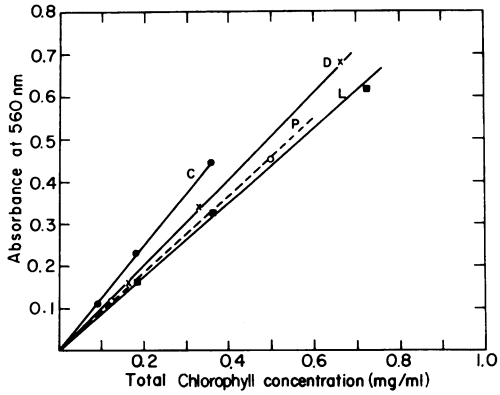

FIG. 2. *A* data for four plant species (corrected for nonspecific light absorption as described in the text). Concentrated chloroplasts were put in a cylindrical cell of 0.1-cm optical path in the integrating sphere and *A* was measured as a function of concentration. C, *C. brevipes;* D, *D. meteloides;* P, *P. emoryi;* L, *L. sparsiflorus.*

[5] Butler (9) estimated $\alpha_1 \simeq 0.3$ in this wavelength range and, therefore, $\alpha_2 \simeq 0.7$, with the possibility of underestimation for α_1 and, therefore, overestimation for α_2.

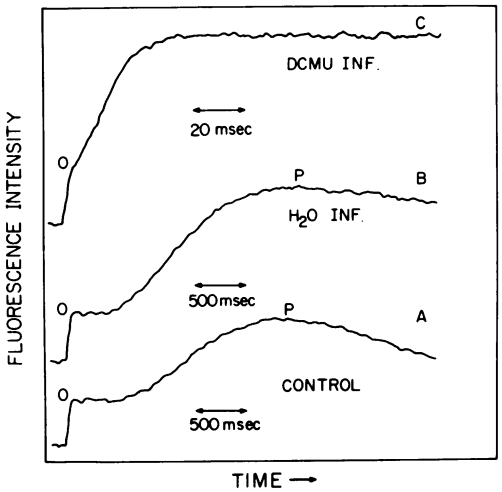

FIG. 3. Fluorescence induction traces for spinach (*S. oleracea*). A, control leaf a few min after harvest; B, same as in A, but infiltrated with water; C, same as in A, but infiltrated with 10 μM DCMU. Light intensity, ~7 nE cm^{-2} s^{-1}. P, peak.

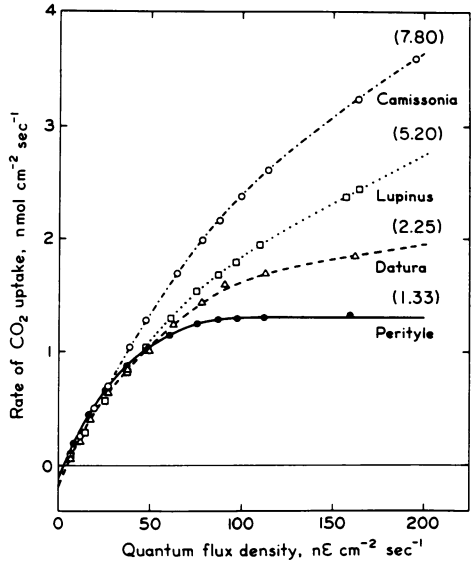

FIG. 4. The rate of photosynthesis (CO_2 uptake) as a function of light intensity for leaves of *C. brevipes, L. sparsiflorus, D. meteloides,* and *P. emoryi.* Measurements of photosynthesis were made at 20 C in normal air (330 μbar CO_2 pressure and 21% O_2). Light was in the wavelength range 400 to 700 nm. The absorbed light intensity was estimated from the incident light intensity and the per cent absorption, measured with a detector of flat spectral response with regard to photon flux. Numbers in parentheses indicate the extrapolated saturation rates.

time (Fig. 3C). This short time usually indicates that RC_{II} alone are involved in the reaction described by equation 1. The fluorescence ultimately reaches a maximal steady level (F_{max}). The control and water-infiltrated leaves (Fig. 3, A and B) exhibit much slower transients. The slow rise to a peak point (P) (Fig. 3) reflects a reduction of a large pool of electron acceptors (40). The subsequent decline to a steady level indicates a complex process involving the interaction of the two photosystems on the level of electron transport and "spillover" of excitation (18). The fluorescence at the peak point (P) (Fig. 3) was usually below F_{max} (as obtained with the DCMU-infiltrated leaves), particularly when the dark adaptation was short. It approached F_{max} for long (sometimes ~1 h) dark adaptation. We also noticed the difference between the fluorescence kinetics of control (Fig. 3A) and water-infiltrated leaves (Fig. 3B), which could be partly due to optical differences (infiltrated leaves scatter the light much less; see below for the effect of scattering) but could be due partly to the direct effect of added water. In the last case, the P → S decline phase was less pronounced.

It could be argued that water (plus DCMU) infiltration might impair or change the primary PSII reaction. This is highly unlikely, however. The F_0 level of fluorescence is much the same as with an intact leaf. The parameter $1 - (F_0/F_{max})$, indicating the quantum yield of the photochemsistry, is usually high in DCMU-infiltrated leaves. (It was equal or even larger than from isolated chloroplasts). Similar values for this parameter could be obtained with intact leaves when long dark adaptation times were given and F_{peak} was substituted for F_{max}.

Fluorescence transients, such as shown in Figure 3C, were used to calculate the induction time and, thereby, PSII PSU size, according to equation 8.

STUDY OF FOUR DESERT PLANTS: CORRELATION OF PSII PSU SIZE AND PHOTOSYNTHETIC CAPACITY

To see whether our numbers for the PSII PSU size were meaningful, a thorough study was made looking for correlation between PSII PSU size as obtained here, PSI PSU size (from P700 measurements), and maximal photosynthetic rates. Four species of markedly different photosynthetic capacity were chosen for the study here.

Figure 4 shows data for the response of net CO_2 uptake per unit leaf area as a function of the absorbed quantum flux density for leaves from each of the four species. *C. brevipes* possessed a rate of photosynthesis nearly 3 times of that for *P. emoryi* and was not light-saturated at the highest quantum flux density used (180 nE cm^{-2} s^{-1}). *L. sparsiflorus* and *D. meteloides* were intermediate between these extremes, with regard to the rate of photosynthesis achieved as well as to the shape of the response curve. All four species exhibited very similar quantum yields of photosynthesis at low light intensities (initial slopes of the response curves).

Measurements of the effect of CO_2 concentration on the rate of photosynthesis revealed that all four species had similar compensation points. Photosynthetic rates were stimulated to a similar (about 30%) percentage by saturating CO_2 concentrations, compared to the ambient (≈250 μbar intercellular) levels (Fig. 5).

Percent light-absorption values and Chl/unit area in the leaves are shown in Table I. With the exception of *P. emoryi,* the leaves of all the plants had similar values of percent absorption and Chl *a/b* ratios were similar for all the species.

Specific leaf weight and nitrogen content of the leaves of the four plants were also determined (Table I). Although the four species possessed different fresh weights per area, the dry weights were very similar, with the exception of *C. brevipes* which was about 50% greater. *L. sparsiflorus* had the greatest percentage of its leaf dry weight as nitrogen, whereas *C. brevipes* possessed the highest concentration of nitrogen on the area basis. It should be noted that the parameter of mg N cm^{-2} corresponded to the photosynthetic capacity of the plants.

Inspection of fluorescence induction curves, obtained in presence of DCMU (Figure. 6) shows very distinct differences in the induction times. Thus, *P. emoryi* required a shorter period of time to achieve the maximal level of fluorescence, indicating that it has more Chl serving the reaction centers of PSII that *C. brevipes,* which required a substantially longer period of time to reach the F_{max} level of Chl fluorescence. *L. sparsiflorus* showed kinetics closer to those of *C. brevipes,* whereas *D. meteloides* showed kinetics closer to those of *P. emoryi.* Thus, there was a close correspondence between the fluorescence rise kinetics and photosynthetic capacity.

The main purpose here was to relate the photosynthetic satu-

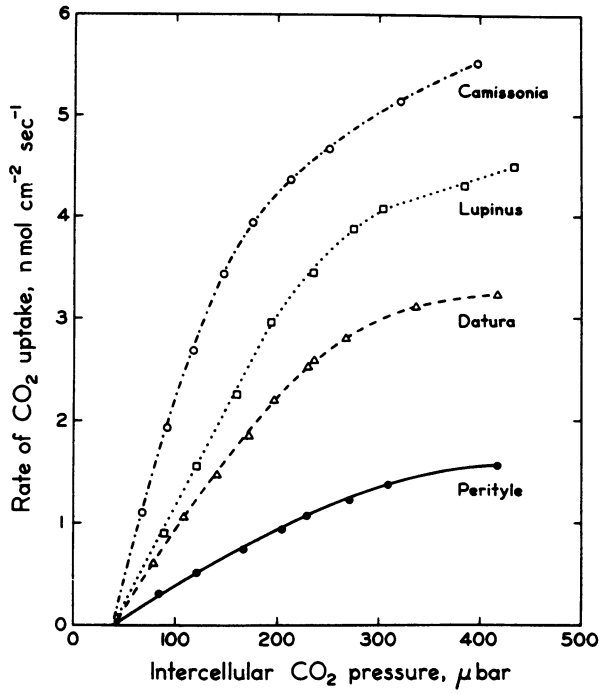

FIG. 5. Response of photosynthesis to CO_2 concentration for leaves of the four plant species. CO_2 uptake was measured in 21% O_2 at a leaf temperature of 20 C and with a quantum flux density of 180 nE cm^{-2} s^{-1}.

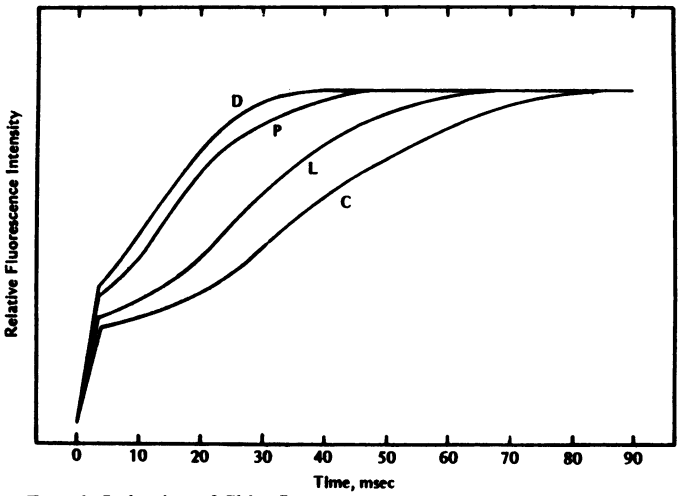

FIG. 6. Induction of Chl *a* fluorescence at room temperature for leaves of *C. brevipes (C), L. sparsiflorus (L), D. meteloides (D),* and *P. emoryi (P).* Detached leaves were vacuum-infiltrated with 20 μM DCMU prior to the measurement. The excitation wavelength was 560 nm; fluorescence emission was monitored at 685 nm.

ration rates and the concentrations of RC_{II}, as obtained by the fluorescence method. From plots of rate^{-1} *versus* light intensity^{-1} using the data of Figure 4 and linear extrapolation to zero reciprocal light intensity, the maximal rate was found for each species and was expressed in terms of unit area or per Chl (from the known Chl per unit area). This rate was further corrected to CO_2 saturation value from the data of Figure 5. The concentrations of RC_{II} were calculated from the fluorescence induction according to equation 7; the details of the calculations are summarized in Table II.

Figure 7 presents the relation between the reaction centers density of PSI and II and the photosynthetic rates. The estimation of the density of the RC_{II} made by the fluorescence method correlates well with the photosynthetic rates, having a linear relationship which extrapolates to the origin. The constant ratio between the photosynthetic rate and the concentrations of the RC_{II} is consistent with a model in which the limiting enzymes(s) (E) has a constant stoichiometric ratio to the reaction centers of PSII and has similar turnover time (σ). In a simple approach, one may write the photosynthetic rate as proportional to the concentration of E with a proportionality constant equal to the reciprocal of the turnover time (σ). Thus one obtains:

$$\left(\frac{\text{rate}}{RC_{II}}\right)^{-1} = \left(\frac{\text{rate}}{(Chl)}\right)^{-1} \cdot \frac{(RC_{II})}{(Chl)} = \sigma \cdot \frac{(RC_{II})}{(E)} \qquad (10)$$

From the data in Figure 5, a similar value for $\sigma \cdot (RC_{II}/E)$ was calculated for the four species being around 32 ± 5 ms (Table II). This is close to the turnover time in photosynthesis as determined by short saturating flashes [*e.g.* around 20 ms in *Chlorella* (13)], suggesting a ratio of E/RC_{II} of the order of unity. A similar correlation between photosynthetic rates and PSU sizes, determined by indirect methods, was obtained previously for few cases (28, 39).

The correlation above gives an indirect support to the initial assumption that the α_2 factor does not vary to a significant extent. Also, these plants had similar Chl *a/b* ratios. It seems that PSII PSU size and Chl *a/b* ratio are not obligatorily related. It was observed (2, 26, 27, 38) that there is a difference in PSU size resulting from differences in the amount of the light harvesting Chl *a/b* complex, with a concomitant difference in the Chl *a/b* ratio. In our case, however, there must be a proportional change in the total number of all light-harvesting Chl molecules rather than the light-harvesting Chl *a/b* protein alone.

In contrast to the good correlation of photosynthetic rates and RC_{II}, there is apparently no correlation between photosynthetic rates and PSI reaction centers (P700) (Fig. 7). There are a few reports in the literature showing correlation of photosynthetic rates and P700 (29, 37) but also some that show a lack of such correlation (23, 30). This failure may arise from two different causes. At first, we thought of the possibility of inactivation of the P700 during chloroplast isolation and subsequent treatments. However, because we usually found high concentrations of P700, it is perhaps probable that only a fraction of all P700 is actively connected to PSII, as already has been suggested (16). We cannot at this time distinguish between these possibilities or assess their relative contributions to the apparent results. It may appear as if *C. brevipes* has substantial P700 inactivation, whereas *P. emoryi* has a large percentage of its P700 not actively involved in photosynthesis. However, our results can be explained easily on the sole basis that the concentration of PSI reaction centers is much less variable with no obligatory relation to RC_{II} and that the electron transport through them is not limiting.

In conclusion, the Chl fluorescence measurements gave values of PSU sizes and densities which were in quantitative agreement with the photosynthetic capacities of the four desert plants. It is quite possible that, in the reported cases of the correlation of rate and P700 (29, 37), the (unmeasured) concentration of RC_{II} also changes with the same general trend, as indeed was documented in one case (24).

VARIABILITY OF PSII PSU SIZE

Having gained confidence in the analysis of the fluorescence induction, we applied it to a large arbitrary variety of species under normal growth conditions. We found that the ratio of total Chl/RC_{II} has considerable variation. Table III gives a list of numerical values for some of the species. Again, the parameter which changed considerably in these measurements was the fluorescence induction time. The F_0/F_{max} ratios, ϵ_i, and Chl *a*/Chl *b*

Table I. *Leaf Characteristics of C. brevipes, D. meteloides, L. sparsiflorus, and P. emoryi*

Species[a]	Leaf Absorbance[b]	Chl	Chl *a/b*	Fresh Weight	Dry Weight	Nitrogen	Nitrogen
	%	$\mu g\ cm^{-2}$	*ratio*	mg/cm^2		%	mg/cm^2
C. brevipes	0.82	55	3.80	34.19	6.20	3.73	0.231
L. sparsiflorus	0.82	59	3.85	42.68	4.03	4.48	0.182
D. meteloides	0.86	52	3.74	27.64	4.37	2.29	0.100
P. emoryi	0.76	34	3.80	36.14	4.08	2.18	0.084

[a] Species ordered according to decreasing photosynthetic capacity.
[b] Measured with respect to the total white light, of spectrum between about 400 and 700 nm, with a detector of flat response with respect to quanta flux.

Table II. *Comparison of Leaf Characteristics from Fluorescence Induction and CO_2 Fixation Rates*

Species	F_0/F_{max}	ϕ_2 (Calculated)	α_2 (Assumed)	RC_{II}/Chl (calculated)	PSII PSU Size	Rate CO_2 Fixation/ Leaf Area[a]	Chl/Leaf Area	Rate CO_2 Fixation/ Chl	$\sigma \cdot (RC_{II}/E)$[b]
	ratio			$10^3 \times$ *ratio*		$nmol/cm^2 \cdot S$	$nmol/cm^2$	s^{-1}	*ms*
C. brevipes	0.23	0.77	0.5	4.65	215	8.6	61	0.14	33
L. sparsiflorus	0.22	0.78	0.5	2.38	420	5.7	65	0.088	27
P. emoryi	0.21	0.79	0.5	1.43	700	1.5	38	0.039	37
D. meteloides	0.27	0.73	0.5	1.28	780	2.4	58	0.041	31

[a] The saturated rates were calculated by hyperbolic linear extrapolation to infinite light intensity (plotting 1/rates *versus* 1/intensity) of the data in Figure 4, allowing certain increase for CO_2 saturation estimated from Figure 5.
[b] Calculated using Equation 10.

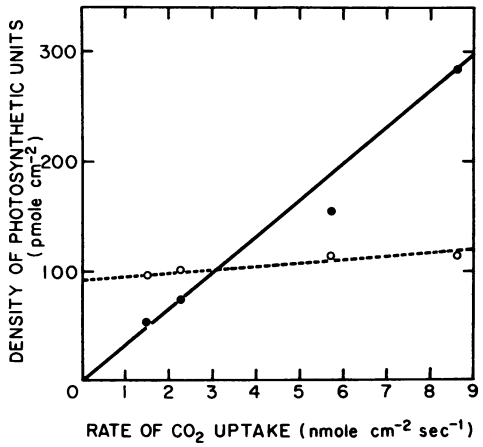

FIG. 7. The density of PSII and PSI (P700) reaction centers as a function of the maximal rate of CO_2 fixation. (●——●), RC_{II}; (○- - -○), P700.

Table III. *PSU Sizes for Various Species*

Species	Chl/RC_{II}
	ratio
Ambrosia camisonis	197
Encilia farinosa	219
Erigonum latifolium	227
Phacelia crenuleta	263
Encilia californica	293
Atriplex sabulosa	328
Ranunculus californica	350
Euphorbia forbesii	395
Pisum sativum var. Laxton Progress #9	420
Atriplex lentiformis	446
Spinacia oleracea	450
Nicotinia tabacum	510

ratios were much less variable.

In contrast to the variation among plant species, there are only limited variation (about ±10% around some average value) when leaves from the same species were examined. This last result stands in contradiction to the report of Schmid and Gaffron (32, 33). They made an extensive study of photosynthesis in flashing light, which is thought to give a measure of the concentration of the reaction centers (although unable to differentiate between PSI and II). Their results were strange and unexplainable in that any given sample of the same plant gave different numbers of considerable variation grouped around an array of specified values in a range between about 100 to 8,000 (total Chl/reaction centers). There are many ways by which the flash method, as utilized in references 32 and 33, can be criticized. Without going into this, we believe that Schmid and Gaffron's (32, 33) results reflect complications in their experimental approach, such as the attenuation of the flash intensity through the leaf as well as uncontrolled dark CO_2 fixation processes, depending on light due to enzyme activation and stomatal opening. Indeed, some of these complications did not appear in the flash measurements on algae (33) which gave constant numbers.

CRITICAL ANALYSIS OF FLUORESCENCE INDUCTION TECHNIQUE

A somewhat more detailed examination of several aspects of the fluorescence induction technique in leaves and possible pitfalls follows.

Test of Equation 7 by Use of Different Wavelengths. As outlined above, the use of actinic wavelengths having large extinction coefficients (ϵ_i) introduce errors in determining the PSU size by equation 5. This is also true for observation of fluorescence at wavelengths of low extinction coefficients (ϵ_f). In spite of this, many previous studies on fluorescence induction have been made at such wavelengths, without using the correction given in equation 7.

To see whether our theoretical predictions are observed experimentally, we compared results for fluorescence induction times for various actinic wavelengths when fluorescence was measured either at 685 or 725 nm. Table IV (top half shows the results of

Table IV. *Effect of Actinic and Emission Wavelengths on Fluorescence Induction Time*

Verification of the assumptions leading to Equation 7 by comparison of induction times for different wavelengths of excitation (λ_i) and two wavelengths of fluorescence (λ_f) corresponding to the peak (685 nm) and to the tail (725 nm) of the fluorescence spectrum; ϵ_i/ϵ_f is estimated from *A* measurement in the integrating sphere. ϕ_2 is estimated from $1 - F_0/F_{max}$. $\bar{\tau}$ is the actual experimental value for the induction time. $\bar{\tau}_{cor}$ is obtained from $\bar{\tau}$ by calculation to equal values of absorbed light as for 550 nm. $\bar{t}_0$ is the calculated induction time contributed by the upper surface (*i.e.* for a hypothetical very thin sample). This value should be the same for all wavelengths in the same column provided that all other parameters are equal. $\bar{\tau}_{cor}$ (calculated) is the calculated induction time for the case where ϵ_i/ϵ_f is very large (in the bottom part of the table) using either equation 6A (for 550 nm) or equation 7A for other wavelengths and the values of $\bar{t}_0$ from the top part of the table. The values of $\bar{\tau}_{cor}$ (calculated) should be compared to the corresponding values of $\bar{\tau}_{cor}$. In this experiment, the detector was placed at an angle θ so that $\cos\theta \sim 0.8$, and the experimental material was spinach leaf.

Wavelengths		ϵ_i/ϵ_f	ϕ_2	I_{inc}	$\bar{\tau}$	$\bar{\tau}_{cor}$	$\bar{t}_0$	$\bar{\tau}_{cor}$ (Calculated)
λ_f	λ_i							
nm								
685	550	0.145	0.64	16.1	21	21	19	
	503	0.64	0.64	10.5	17.2	50	33	
	462	1.07	0.64	5.1	14.6	34	18	
	433	1.32	0.65	3.2	15.7	29	15	
725	550	~10	0.54	16.1	27	27		29
	530	~40	0.56	10.5	26	75		90
	462	~70	0.54	5.1	22	51		52
	433	~90	0.55	3.2	21	38		42

such an experiment. For proper comparison, the observed induction times ($\bar{\tau}$) had to be corrected for the difference in both incident light and *A* so that their values will be compared on the basis of equal light absorbed. This was done by use of equation 6, taking into account that the absorbed light intensity is proportional to the product of the extinction coefficient [$\epsilon_i(\lambda)$] and the incident intensity (I_0). Comparing all the data to that of 550 nm for the effect of equal absorbed intensities, values were obtained for "corrected" experimental induction time ($\bar{\tau}_{cor}$). As expected from equation 7, all other wavelengths resulted in much longer (corrected) induction times compared to the standard actinic wavelength (λ_i = 550 nm; λ_f = 685 nm). From the observed values of $\bar{\tau}_{cor}$, it was possible to calculate $\bar{t}_0$, according to equation 7, which should give the same number for all actinic wavelengths. Indeed, for three wavelengths (550, 462, 433 nm), the values were quite similar (17 ± 2 ms). For 503 nm, the induction time, however, was exceptionally long. This may be the result of some other reason, such as inefficiency (*e.g.* smaller α_2) due to increased light absorption by carotenoid pigments, relative to Chl.

When the fluorescence was observed at a long wavelength (725 nm), it had an observed induction time significantly longer compared to the induction time of fluorescence observed at the peak (685 nm) (Table IV, compare the values for $\bar{\tau}$ or $\bar{\tau}_{cor}$ for the same exciting wavelength but for different emission wavelengths). Theory predicts that the apparent kinetics of long wavelength fluorescence from the entire leaf when $\epsilon_f \ll \epsilon_i$ is significantly slower than the kinetics for the idealized situation of a thin section of the leaf exposed to the same incident intensity. This is derived in Appendix II and demonstrated in Figure 8. The extent of the increase in apparent induction time when the fluorescence is measured at 725 nm is nearly the same as that estimated from the mathematical treatment and from the values for $\bar{t}_0$ (*cf.* Appendix I, equations 6A and 7A). This is seen by comparison of the calculated and observed values of the corrected induction times ($\bar{\tau}_{cor}$) [Table IV, bottom half; compare $\bar{\tau}_{cor}$ and $\bar{\tau}_{cor}$ (calculated)]. Considering the above effect, it is evident that the spectral composition of the fluorescence should vary in time. Such variation was observed by Schreiber and Vidaver (34) but interpreted as arising due to real processes such as changes in distribution of energy between the two photosystems. This should be therefore reconsidered.

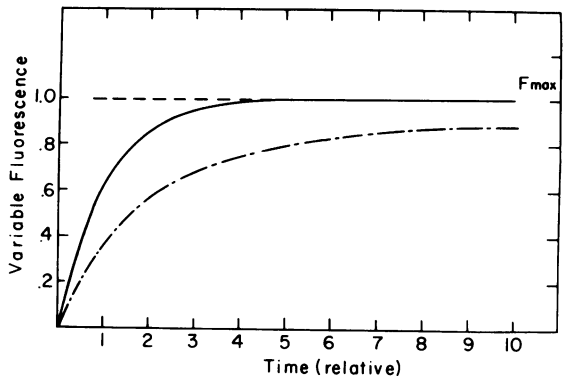

FIG. 8. Comparison of the theoretical expectation of a fluorescence induction curve from an idealized leaf of infinite optical path length when $\epsilon_f/\epsilon_i \rightarrow 0$ (bottom curve) to the contribution of the induction from the front surface alone, realized when $\epsilon_i/\epsilon_f \rightarrow 0$ (top curve). Both are normalized to the same extent.

Ratio of $1 - (F_0/F_{max})$ as Indicator for ϕ_2. In most of the plant species tested, the ratio of F_0/F_{max} was usually less than 0.3, implying that ϕ_2 is higher than 0.7. There were a few special cases where the ratio F_0/F_{max} was quite high (*i.e.* >0.5). One must bear in mind that part of the observed F_0 does not necessarily reflect the quenched fluorescence state of PSII and may contain other contributions (*i.e.* PSI, nonconnected pigments, damaged units of PSII). In certain algae (*e.g.* blue-greens) the background fluorescence was found to be usually very high (F_0/F_{max}, close to 1). In such cases, application of equation 8 is not appropriate, unless an independent way would be found to distinguish between the background and the truly PSII active fluorescence. A possible approach to assay how much F_0 is "dead" is to analyze the lifetime of fluorescence and its relation to the fluorescence intensity during the induction period (22, 25). This last approach should be developed as an additional tool in conjunction with the present method.

Fortunately, healthy higher plants are probably amenable to our analysis, having mostly small F_0/F_{max} ratios. An arbitrary criterion, at present, would be to use equation 8 as far as F_0/F_{max} is less than or equal to about 0.7 and to discard all the other cases.

Effect of Light Scattering in Leaf: Comparison of Leaves to Chloroplasts. Our starting point that light is attenuated in passing through the leaf following a simple Beer-Lambert law (Appendix I) was probably too simplistic. Evidently, the leaf is a much more complicated optical sytem (8), mainly because of the abundance and heterogeneity of light-scattering elements. It seems that there are three main ways that light scattering modifies the light flux distribution through its optical path: (*a*) back reflection of light from various deeper cross-sections of the leaf adds to the incident light intensity at the top part of the leaf (Thus, the light intensity is stronger than anticipated on the basis of incident light measurements only.); (*b*) direct reflection from the utmost top surface (*e.g.* the waxy cutin, leaf hairs, and epidermal cells) decreases the incident light intensity on the first layer of chloroplasts); (*c*) the angular distribution of light is changed by the scattering from an initial vertical direction to various shallower angles, increasing the effective optical path. This effect can be regarded as equivalent to an increase in the effective extinction coefficient (due to the increase in the average time of light passage through a given leaf layer). Effects *a* and *c* contribute to increased light absorption

and, hence, to a shortening of the fluorescence induction time, whereas effect *b* contributes to the opposite. The following experiments show that in general all these scattering effects are insignificant in infiltrated leaves.

An artificial demonstration of the combined effects *a* and *c* was made on chloroplasts suspension into which increasing various concentration of light scattering material was added. Measurements of fluorescence induction in such suspension (Fig. 9a) showed that the induction time was gradually decreased as the scatterer concentration increased. The amount of scattering from these suspensions was specified in a quantitative way be measuring the total reflection and transmission in an integrating sphere and by correlating them to the fluorescence induction time (Fig. 9b).

Assuming that the scattering effects are relatively small for a normal chloroplast suspension (*i.e.* without any additional scatterer), it was of interest to check whether induction times from infiltrated leaves and isolated chloroplasts from the same kind of leaves will agree. In such a case this will imply that scattering effects in the infiltrated leaves are not so important. Table V presents such a comparison, showing usually an agreement between chloroplasts and leaves. This result comes to a better focus

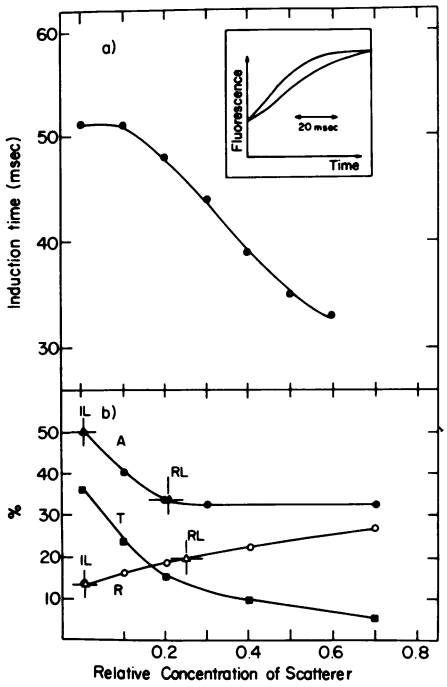

FIG. 9. a, the effect of addition of varying amounts of neutral scatterer on the induction time of fluorescence in a pea chloroplast suspension. Inset, fluorescence induction traces without scatterer (bottom curve) and with the maximal scatterer concentration (top curve). The concentration of the scatterer is expressed as the fractional volume. Chl concentration, 440 μg/ml; light intensity, 12.5 nE cm^{-2} s^{-1}. Scatterer used was concentrated milk with a 1-mm path cuvette. b, optical parameters of a pea chloroplast suspension, compared to a pea leaf, measured at 550 nm in the integrating sphere in a 1-mm path cuvette. The Chl concentration per unit area in the chloroplast suspension was adjusted to match that of a leaf (44 μg Chl/cm^2, the same as above). A, per cent light transmitted and reflected from the sample; R, per cent reflection; T, per cent transmission, (A = R + T). Reflection was measured by placing a black tape at the bottom of the sample so that light could not be transmitted but only reflected. Transmission was computed from A and R. The points correspond to the chloroplast measurements as the concentration of the neutral scatterer varies. The triangle points with "radiating arms" correspond to the leaf measurements and were placed on the corresponding chloroplast suspension curves with the appropriate values for A and T. IL, infiltrated leaf, RL, regular leaf.

Table V. *Comparison of Induction Times from Leaves and Chloroplasts*

Experiments comparing leaves and chloroplasts were done with the same intensities. Chloroplasts remained in their grinding medium. Light intensities were not measured but were estimated between 5 to 15 nE cm^{-2} s^{-1}.

Sample	Induction Time	
	Chloroplasts	Leaf
	ms	
P. sativum grown in intermittent light	100 ± 10	83 ± 10
P. sativum grown in intermittent light followed by continuous light[a]	34 ± 2	31 ± 2
P. sativum grown normally[a]	25 ± 1	25 ± 1
S. oleracea[b]	20.6 ± 0.3	20.7 ± 0.3
Nicotinia tabacum	53 ± 2	50 ± 2
Arcototis stoechadifolia	56 ± 2	42 ± 2

[a] This species was purposely chosen since its photosynthetic unit size is largely changed depending on the growth conditions (2).

[b] This experiment was analyzed by a computer, giving a better estimate for the induction time.

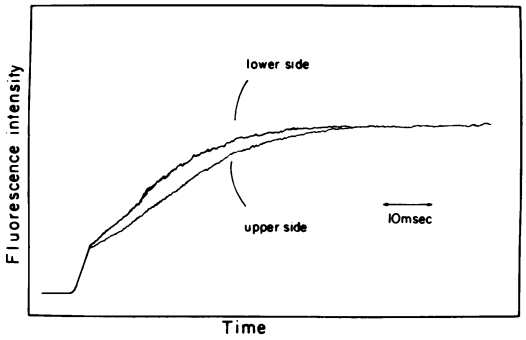

FIG. 10. Fluorescence induction curves of two pea leaf sides: upper curve, bottom side; lower curve, top side. Exciting light intensity, ∿10 nE cm^{-2} s^{-1}.

when also the total reflection and transmission parameters of intact and infiltrated leaves are compared to those of isolated chloroplasts (*cf.* Fig. 9b). Although an intact leaf is equivalent to a chloroplast suspension with an additional scatterer, the infiltrated leaf gave essentially identical reflection and transmission values as a normal suspension of isolated chloroplasts (*i.e.* without additional scatterer). One can conclude that, when water fills all the intracellular spaces, the scattering effect is very much reduced and, for our purposes, largely insignificant.

In the studies above, there were, however, some isolated exceptions of somewhat shorter induction times in leaves compared to isolated chloroplasts (Table V). These cases are evidently due to increased scattering. The species *Arcototis stoechadifolia* is an example of such a case. Its leaf has a strong whitish hue which indicates a high ratio of scattering elements to pigments. The same situation occurs also for pea leaves grown in intermittent light. Such cases are usually quite isolated.

It was reported (35), that the induction time obtained from the underside of a DCMU-infiltrated[6] leaf is somewhat shorter compared to that obtained from the upperside. This was repeated by us again (Fig. 10). Presumably this effect can be traced to a

[6] For leaves which were not treated with DCMU, there were much larger changes in the fluorescence induction times [time to attain peak P (Fig. 3)] from the upper and under sides (35). These changes reflect probably real differences in the plastoquinone pool sizes, caused by the adaptation to the different light environments on the two sides of the leaf (5, 6, 35).

considerable scattering in the leaf underside, as compared with the leaf upperside. Indeed, the underside is generally whitish, indicating an abundance of scattering elements. It had been suggested (35) that the increased scattering decreases the light intensity and consequently lengthens the induction time, [*i.e.* considering only effect *b* of scattering as described above]. The difference in induction times was therefore explained in terms of different PSU sizes of PSII for the opposite sides of the leaf (35). However, as indicated above, this explanation is not necessary; it is quite possible that effects *a* and *c* of scattering enhance the effective light intensity at the underside.

Appendix I: Calculation of fluorescence induction time from a leaf, assuming Beer-Lambert attenuation law for the exciting and fluorescence light (*cf.* Fig. 1).

The equation for the exciting intensity at depth l is:

$$I(l) = I_0 \cdot 10^{-\epsilon_i c l} \tag{1A}$$

where I_0 is the incident intensity, the wavelength is λ_i, the extinction coefficient corresponding to this wavelength is ϵ_i, and c is the total Chl concentration (molar).

The fluorescence created at depth l from a layer of thickness dl is proportional to $I(l)$, but the portion viewed by the detector is further attenuated by the factor $10^{-\epsilon_f c l/\cos\theta}$. Hence:

$$F(l)dl = k \cdot I_0 \cdot 10^{-\epsilon_i c l} \cdot 10^{-\epsilon_f c l/\cos\theta} dl \tag{2A}$$

where k is a proportionality factor.

The induction time $[\bar{t}(l)]$ contributed by the layer at depth l is according to equation 6 (*cf.* main text) equal to:

$$\bar{t}(l) = \frac{\bar{t}_0 I_0}{I(l)} \tag{3A}$$

To obtain the measured induction time, one has to average the total contributions of $\bar{t}(l)$ weighted according to their contribution to the total fluorescence contribution. Thus:

$$\bar{\tau} = \frac{\int_0^d \bar{t}(l)F(l)dl}{\int_0^d F(l)dl} \tag{4A}$$

After proper substitutions of equations 1A to 3A into equation 4A, one obtains:

$$\bar{\tau} = \bar{t}_0 \cdot \frac{1 - 10^{-\epsilon_f cd/\cos\theta}}{1 - 10^{-(\epsilon_i cd + \epsilon_f cd/\cos\theta)}} \cdot \left(1 + \frac{\epsilon_i}{\epsilon_f}\cos\theta\right) \tag{5A}$$

Application of Equation 5A to Case of Low Extinction of Actinic Light and High Extinction of Fluorescent Light. $\bar{\tau}$ is expressed as a product of three factors: $\bar{t}_0$ and two correction factors by which it is multiplied.

The first correction factor is very nearly 1 under all practical circumstances. To see this, one has to recognize that $c \cdot d$ is the Chl surface concentration in mol/1,000 cm^2, which is usually in the range of 1 to 5 $\times$ 10^{-5}. The approximate extinction of the wavelengths used by us are: ϵ_f (for 685 nm), $\sim 10^5$; ϵ_i (for 550 nm), $\sim 10^4$. From these numbers, it turns out that the first factor is always bigger than 0.99 for all wavelengths (mostly even 0.999) but less than 1. This means that the limits of integration in equation 4A can be taken practically between 0 and ∞. This leads directly to equation 7 (see main text).

The second correction factor $[1 + (\epsilon_i/\epsilon_f)\cos\theta)]$ approaches 1 as ϵ_i becomes much smaller compared to ϵ_f and also as θ increases, which is an ideal condition. In our case, this situation is approached and $(\epsilon_i/\epsilon_f)\cos\theta \approx 0.075$. Thus, the error introduced by taking $\bar{\tau}$ as equal to $\bar{t}_0$ amounts only to about 7.5%.

Case of Low Extinction of Fluorescent Light. For comparison, we consider also the opposite case that ϵ_f is very small (*e.g.* when fluorescence is measured at its far-red side, $\epsilon_f \sim$ 725 nm). In this case, one can approximately write $1 - 10^{-\epsilon_f cd/\cos\theta} \approx 2.3\ \epsilon_f cd/\cos\theta$. Neglecting, in this case, ϵ_f compared to ϵ_i, equation 5A is approximated by:

$$\bar{\tau} = \bar{t}_0 \cdot \frac{2.3\ \epsilon_i cd}{1 - 10^{-\epsilon_i cd}} \tag{6A}$$

Thus, the total observed induction time when $\epsilon_f/\epsilon_i \to 0$ is related to the induction time from the upper surface only ($\bar{t}_0$) by the factor $2.3\ \epsilon_i cd/(1 - 10^{-\epsilon_i cd})$, which is a function of the absorption properties of the incident beam only.

Although Equation 6A should be applied strictly in all cases, its practical use in the above form is limited to a case where the actinic light is not attenuated radically (*e.g.* at 550 nm, where the observed optical density of an infiltrated leaf is around 0.4). When the actinic light is in effect totally absorbed (around 430 nm), there is a practical problem related to the accuracy of measurement of the fluorescence-induction kinetics. In such a case, one does not have the precision to observe the full fluorescence induction development; as Appendix II shows, much of the contribution to $\bar{\tau}$ appears at the very long tail at the end of the induction. Such a tail is often buried under noise and also changes very slowly (approximately like $1/t$, *cf.* Appendix II) and causes the false impression that the induction phenomenon is over, before it really is. This tail is caused by the remains of the attenuated actinic light beam, at a large depth, which, although contributing little to the fluorescence amplitude, contribute very considerably to $\bar{\tau}$ (*cf.* equation 3A). Such a tail is actually "missed" by the detection system and, hence, a proper upper limit must be introduced to the integral of equation 4A which is less than $l = d$. It is set at a point where the light is attenuated to a degree where its contribution to fluorescence is below the accuracy of detection. A good guess for such a limit, although quite arbitrary, is to place it where the light is attenuated to about 10% of its incident value. This corresponds to an attenuation of optical density = 1. Therefore, we substitute, in equation 6A, the value 1 instead of $\epsilon_i cd$, which leads to:

$$\bar{\tau} \sim 2.5\ \bar{t}_0 \tag{7A}$$

with $\epsilon_f/\epsilon_i \to 0$ $\quad \epsilon_i cd = 1$ (Corresponding to 10% accuracy).

Appendix II: Dependence of fluorescence intensity on time at two emission wavelengths.

λ_f. Where Fluorescence Is not Attenuated at All ($\epsilon_f/\epsilon_i \ll 1$). Besides the assumptions made in Appendix I, we also assume that the time dependence form of each contribution to the induction is exponential; this may be not quite exact (14), but it is sufficient for the following illustration. For the case that the fluorescence is not attenuated, the contribution to the variable fluorescence from each layer (l) may be written:

$$F(l)dl = kI(l)(1 - e^{-\beta I(l)t})dl \tag{8A}$$

This equation expresses the fluorescence dependence on time as a decreasing exponential containing the factor $I(l)t$ with a specific rate constant (β) which depends on the pool size of the reaction centers. The amplitude of each contribution is proportional to $I(l)$, with a proportionality constant (k). Writing $I(l) = I_0 10^{-\epsilon_i c l}$, the total variable fluorescence is given by integration on l. The integration is better carried out by the replacement of variables. Writing $dl = -(1/2.3\ \epsilon_i c)(dI/I)$,

$$F = \int_0^d F(l)dl = \frac{k}{2.3\ \epsilon_i c} \int_{I_0 \cdot 10^{-\epsilon_i cd}}^{I_0} (1 - e^{-\beta I t})dI \tag{9A}$$

It is customary to normalize the maximal variable fluorescence to 1; this is done by adjusting the proportionality coefficient k by

equating F to 1 at $t \rightarrow \infty$. The final result is:

$$F = 1 - \frac{1}{I_0(1 - 10^{-\epsilon_i cd})} \cdot \frac{1}{\beta t} [e^{-(\beta I_0 10^{-\epsilon_f c'} t)} - e^{-\beta I_0 t}] \quad (10A)$$

λ_f: Where Fluorescence Has Maximum Attenuation ($\epsilon_f/\epsilon_i \gg 1$). Equation 10A gives the time relation of the (normalized) fluorescence from the entire leaf. This has to be compared with the time dependence of fluorescence obtained only from the top layer, which is nearly the same as fluorescence obtained when $\epsilon_i/\epsilon_f \ll 1$. For this case, it is convenient to make a substitution to a new time variable, $T = \beta I_0 t$. The normalized fluorescence from the top layer (denoted by F') is expressed by:

$$F' = (1 - e^{-T}) \quad (11A)$$

On the other hand Equation 10A is expressed now as:

$$F = 1 - \frac{1}{(1 - 10^{-\epsilon_i cd})} \cdot \frac{1}{T} [e^{-(10^{-\epsilon_f cd} T)} - e^{-T}] \quad (12A)$$

To show the relation between F and F', it is possible to simplify Equation 12A by assuming that the exciting light is attenuated considerably at the other side of the leaf so that $10^{-\epsilon_i cd} \approx 0$. In this case, Equation 12A is approximated to:

$$F = 1 - \frac{1}{T}(1 - e^{-T}) \quad (13A)$$

Comparing F to F', one observes that F tends to 1 not exponentially but, rather, in a much weaker way. At long times, F is even further approximated to $(1 - 1/T)$. It is clear, therefore, that two fluorescence wavelengths, one at the peak and one at the far red side tail, show quite different kinetic responses (*cf.* text). This is demonstrated by Figure 6, which compares the two functions, expressed by Equations 11A and 13A.

LITERATURE CITED

1. ALBERTE RS, JD HESKETH, G HOFSTRA, JP THORNBER, RL BERNARD, C BRIM, J ENDRIZZI, RJ KOHEL 1974 Composition and activity of the photosynthetic apparatus in temperature-sensitive mutants of higher plants. Proc Natl Acad Sci USA 71: 2414–2418
2. ARMOND PS, CJ ARNTZEN, JM BRIANTAIS, C VERNOTTE 1976 Differentiations of chloroplast lamellae: light harvesting efficiency and grana development. Arch Biochem Biophys 175: 54–63
3. ARMOND PA, MR BADGER, O BJORKMAN 1978 Characteristics of the photosynthetic apparatus developed under different thermal growth regimes. *In* G Akoyunoglou, and J H Argyroudi-Akoyunoglou, eds, Chloroplast Development. Elsevier-North Holland Biomedical Press, Amsterdam, pp 857–862
4. ARNON DE 1949 Copper enzymes in isolated chloroplasts. Polyphenoloxidase in *Beta vulgaris*. Plant Physiol 24: 1–15
5. BJORKMAN O 1971 Photosynthetic adaptation to contrasting light climates. Carnegie Inst Wash Year Book 71: 82–85
6. BJORKMAN O, NK BOARDMAN, JM ANDERSON, SW THORNE, DJ GOODCHILD, NA PYLIOTIS 1971 Effect of light intensity during growth of *Atriplex patula* on the capacity of photosynthetic reactions, chloroplast components, and structure. Carnegie Inst Wash Year Book 71: 115–135
7. BJORKMAN O, HA MOONEY, J EHLERINGER 1974 Photosynthetic responses of plants from habitats with contrasting thermal environments: comparison of photosynthetic characteristics of intact plants. Carnegie Inst Wash Year Book 74: 743–751
8. BRANDT AN, SV TAGEYEVA 1967 Optical Parameters of Plant Organisms (in Russian). Nauka, Moscow
9. BUTLER WL 1977 Chlorophyll fluorescence: A probe for electron transfer and energy transfer. *In* A Trebst and M Avron, eds, Encyclopedia of Plant Physiology, Springer-Verlag, Heidelberg, pp. 149–166
10. CAHEN D, S MALKIN, S SHOCHAT, I OHAD 1976 Development of photosystem II complex during greening of *Chlamydomonas reinhardi* y-1. Plant Physiol 58: 257–267
11. DUBERTRET G, P JOLIOT 1974 Structure and organization of system II photosynthetic units during the greening of a dark grown *Chlorella* mutant. Biochem Biophys Acta 357: 399–411
12. EHLERINGER J, O BJÖRKMAN 1977 Quantum yields for CO_2 uptake in C_3 and C_4 plants. Plant Physiol 59: 86–90
13. EMERSON R, W ARNOLD 1932 The photochemical reaction in photosynthesis. J Gen Physiol 16: 191–205
14. FORD GA, S MALKIN, DC FORK 1978 Computer-assisted measurements of parameters of the rise curve of fluorescence. Carnegie Inst Wash Year Book 78: 199–201
15. GOVINDJEE, R GOVINDJEE 1975 Introduction to photosynthesis. *In* Govindjeee, ed, Bioenergetics of Photosynthesis. Academic Press, New York, pp. 1–50
16. HAEHNEL W 1976 The ratio of the two light reactions and their coupling in chloroplasts. Biochim Biophys Acta 423: 499–509
17. KOK B 1956 On the reversible absorption change at 705 nm in photosynthetic organisms. Biochim Biophys Acta 22: 399–401
18. LAVOREL J, AL ETIENNE 1977 *In vivo* chlorophyll fluorescence. *In* J Barber, ed, Primary Processes of Photosynthesis, Chap 6. Elsevier, Amsterdam, pp. 203–268
19. MALKIN S, B KOK 1966 Fluorescence induction studies in isolated chloroplasts. Number of components involved in the reaction and quantum yields. Biochim Biophys Acta 126: 413–432
20. MALKIN S, Y SIDERER 1974 The effect of salt concentration on the fluorescence parameters of isolated chloroplasts. Biochim Biophys Acta 368: 422–431
21. MALKIN S, DC FORK, PA ARMOND 1977 Probing photosynthetic unit sizes of leaves by fluorescence-induction measurements. Carnegie Inst Wash Year Book 77: 237–240
22. MALKIN S, D WONG, GOVINDJEE, H MERKELO 1980 Parallel measurements on fluorescence life-time and intensity changes from leaves during the fluorescence induction. Photobiochem Photobiophy 1: 83–89
23. MELL V, H SENGER 1978 Photochemical activities, pigment distribution, and photosynthetic unit size of subchloroplast particles isolated from synchronized cells of *Scenedesmus obliquus*. Planta 143: 315–322
24. MILES CD 1974 Control of the light saturation point of photosynthesis in tomato. Physiol Plant 31: 153–158
25. MOYA I, GOVINDJEE, C VERNOTTE, JM BRIANTAIS 1977 Antagonistic effect of mono and divalent-cations on life-time (τ) and quantum yield of fluorescence (ϕ) in isolated chloroplasts. FEBS Lett 75: 13–18
26. MAKAMURA D, T OGAWA, K SHIBATA 1976 Chlorophyll and peptide compositions in the two photosystems of marine algae. Biochim Biophys Acta 423: 227–237
27. OGAWA T, Y INOUE, K SHIBATA 1974 Chlorophyll *a* forms in mesophyll and bundle sheath chloroplasts of *Zea mays* leaves grown at low light intensity. Plant Cell Physiol 15: 913–918
28. OKABE K, GH SCHMID, J STRAUB 1977 Genetic characterization and high efficiency photosynthesis of an aurea mutant of tobacco. Plant Physiol 60: 150–156
29. PATTERSON DT, JA BUNCE, RS ALBERTE, E VAN VOLKENBURGH 1976 Photosynthesis in relation to leaf characteristics of cotton from controlled and field environments. Plant Physiol 59: 384–387
30. PATTERSON DT, SO DUKE 1979 Effect of growth irradiance on the maximum photosynthetic capacity of water hyacinth *Eichhornia crassipes* (Mart.) Solms. Plant Cell Physiol 20: 177–184
31. PREZELIN BB 1976 The role of peridinin-chlorophyll *a*; proteins in the photosynthetic light adaptation of the marine dinoflagellate *Glenodinium sp.* Planta 130: 225–233
32. SCHMID GH, H GAFFRON 1968 Photosynthetic units. J Gen Physiol 52: 212–239
33. SCHMID GH, H GAFFRON 1971 Fluctuating photosynthetic units in higher plants and fairly constant units in algae. Photochem Photobiol 14: 451–464
34. SCHREIBER U, W VIDAVER 1976 Rapid light induced changes of energy distribution between photosystems I and II. FEBS Lett 62: 194–197
35. SCHREIBER U, R FINK, W VIDAVER 1977 Fluorescence induction in whole leaves: differentiation between the two leaf sides and adaptation in different light regimes. Planta 133: 121–129
36. SHIOZAWA JA, RS ALBERTE, JP THORNBER 1974 The P700 chlorophyll *a* protein. Arch Biochem Biophys 165: 383–397
37. TEERI JA, DT PATTERSON, RS ALBERTE, RM CASTLEBERRY 1977 Changes in the photosynthetic apparatus of maize in response to simulated natural temperature fluctuations. Plant Physiol 60: 370–373
38. THORNBER JP, HR HIGHKIN 1974 Composition of the photosynthetic apparatus of normal barley leaves and a mutant lacking chlorophyll *b*. Eur. J. Biochem 41: 109–116
39. WILD A1969 The size of the photosynthetic unit and its variability in yellow mutants. *In* H Metzner ed, Progress in Photosynthesis Research, Vol 2. H Laupp, Jr, Tubingen (Germany), pp 871–876
40. ZANKEL KL, B KOK 1972 Estimation of pool sizes and kinetic constants. Methods Enzymol 24: 871–876